Characteristics of Deep Convective Clouds, Precipitation, and Cloud Properties of Rapidly Intensifying Tropical Cyclones in the Western North Pacific

by Chian-yi Liu

AGU ADVANCING EARTH AND SPACE SCIENCE

JGR Atmospheres

RESEARCH ARTICLE
10.1029/2022JD037328

Characteristics of Deep Convective Clouds, Precipitation, and Cloud Properties of Rapidly Intensifying Tropical Cyclones in the Western North Pacific

Chian-Yi Liu[1,2,3], Jason Pajimola Punay[2,4], Chun-Chieh Wu[5], Kao-Shen Chung[2], and Putu Aryastana[3,6]

[1]Research Center for Environmental Changes, Academia Sinica, Taipei, Taiwan, [2]Department of Atmospheric Sciences, National Central University, Taoyuan, Taiwan, [3]Center for Space and Remote Sensing Research, National Central University, Taoyuan, Taiwan, [4]Department of Physics, College of Science, Bicol University, Legazpi City, Philippines, [5]Department of Atmospheric Sciences, National Taiwan University, Taipei, Taiwan, [6]Department of Civil Engineering, Warmadewa University, Denpasar, Indonesia

Abstract Toward the understanding of rapid intensification (RI) of tropical cyclones (TCs) in the western North Pacific, the TC's deep convective cloud (DCC), precipitation, and cloud properties in terms of cloud effective radius, optical thickness, and top height from satellite observations are investigated. Mean and radial distributions of the variables at different intensity stages and intensification categories are examined. The relationship indicates that the DCC percentage and temperature, especially their radial distributions, could be used to identify an impending RI regardless of TC intensity. Meanwhile, the mean and radial distribution of precipitation may discriminate RI from non-RI in tropical depression (TD) and tropical storm (TS). The radial distribution of the cloud properties in rapidly intensifying TD and TS also suggest that most of the clouds near the center of the storm has deepened already while those that are far from the center are generally in developing or dissipating stage. Moreover, rapidly intensifying TCs, regardless of their intensities, manifest common DCC, precipitation, and cloud properties characteristics near the TC center. It is to be noted that the different mean and radial distribution characteristics of the variables between initial and continuing stages of RI are inferred to be artifacts of their intensities and RI rates (or radius of maximum wind sizes) rather than whether the TCs are at the onset or 24 hr of RI.

Plain Language Summary We want to know if there are unique features of deep convective cloud (DCC), rain, and cloud properties that can be used to predict the rapid intensification (RI) of a tropical cyclone. RI can be predicted using DCC in all storm categories. Precipitation is also useful in anticipating RI but for weaker storms only. The deep convection, rain, and cloud properties near the center of rapidly intensifying storms suggests that clouds within that region has deepened already as compared to the clouds that far away from the center. All storms that are rapidly intensifying share the same DCC, rain, and cloud properties characteristics near the center. The different characteristics observed at the beginning and at 24 hr of RI are more related to their intensities and intensification rates (or the size of their radii of maximum wind).

Key Points:

- Deep convective cloud's (DCC's) radial distribution can identify an impending rapid intensification (RI), whereas precipitation can be used to anticipate RI in weak tropical cyclones (TCs)
- RI TCs, regardless of their intensities, have common DCC, precipitation, and cloud properties characteristics at the TC center
- Characteristics found in initial and continuing RI are artifacts of their intensities and RI rates (or radius of maximum wind sizes)

Correspondence to:
J. P. Punay,
jppunay@bicol-u.edu.ph

Citation:
Liu, C.-Y., Punay, J. P., Wu, C.-C., Chung, K.-S., & Aryastana, P. (2022). Characteristics of deep convective clouds, precipitation, and cloud properties of rapidly intensifying tropical cyclones in the western North Pacific. *Journal of Geophysical Research: Atmospheres*, *127*, e2022JD037328. https://doi.org/10.1029/2022JD037328

Received 28 JUN 2022
Accepted 25 NOV 2022

1. Introduction

Understanding the mechanisms that control tropical cyclone (TC) intensity changes is crucial for weather forecasters to predict intensification, especially rapid intensification (RI). TC intensification is considered to occur under the following favorable large-scale environmental conditions: warm sea surface temperature (SST), weak vertical wind shear (VWS), high low-to-mid troposphere humidity, and high upper oceanic heat content (Chang & Wu, 2017; Cione & Uhlhorn, 2003; DeMaria et al., 2005; Kaplan & DeMaria, 2003; Kaplan et al., 2010; Mainelli et al., 2008; Wang et al., 2015) or TC heat potential (Pun et al., 2013; Wu et al., 2016). Moreover, a recent study showed that even shallow coastal bathymetry may have contributed in providing favorable conditions for the RI of TC Hato (2007, Pun et al., 2019). In a study in western North Pacific from 2000 to 2011, SST of 28.9°C generally favors TC intensification (Shu et al., 2014). An increase in SST increases the water vapor flux, providing additional low-tropospheric humidity (Črnivec et al., 2016) for condensation, through which latent heat is released. With SSTs higher than 29°C and under weak deep-layer VWS environment of less than 9 m s^{-1}, the probability of RI increases (Wang et al., 2015). On average, however, no significant difference exists

in the environmental conditions between intensifying and rapidly intensifying TCs (Hendricks et al., 2010). This implies that these conditions have limited influence on the rate of TC intensification.

Internal dynamic and thermodynamic processes that operate on subsynoptic scales may be crucial for identifying TCs that undergo intensification and RI. Latent heating, deep convection, and precipitation are among the processes within a storm that are associated with intensity change. Their radial and vertical locations and the degree of symmetry in the inner core are critical factors that affect intensification (Hack & Schubert, 1986; Zipser et al., 2014). Specifically, intensification is more likely when latent heating occurs near the TC's center (Nolan et al., 2007; Simpson et al., 1998). Zagrodnik and Jiang (2014) reported that the most intense latent heating during RI occurs entirely within the 50-km radius from the storm center. The same study found that rapidly intensifying TCs have more axisymmetric distributions of latent heat and precipitation than other intensity change categories.

Precise identification of precursors and responses is critical for determining mechanisms that control RI. According to observations of 37-GHz precipitative ring, the emergence of a ring around TC's center coupled with favorable environmental conditions increases the likelihood of RI (Kieper & Jiang, 2012). Using Tropical Rainfall Measuring Mission (TRMM) precipitation radar (PR), Zagrodnik and Jiang (2014) found that an increase in moderate-to-deep convection starts to be remarkable at least 12 hr after the onset of RI. Deepest cells in the inner core have also been found to develop near or at the end of RI, which suggests that deep convection does not necessarily trigger RI (Nguyen & Molinari, 2012). Several studies consider deep convection a response to RI rather than a trigger (Nguyen & Molinari, 2012; Rogers et al., 2013; Tao & Jiang, 2015; Zagrodnik & Jiang, 2014). Because additional precipitation during the onset of RI mainly results from shallow-to-moderate rain, related studies have asserted that stratiform rain may be a better predictor of RI than deep convection (Tao & Jiang, 2015; Tao et al., 2017). Alvey et al. (2015) further suggested that increasing symmetry of precipitation could be a possible indicator of a RI and an impending RI.

Ruan and Wu (2018) argued that stratiform rains observed through TRMM PR snapshots may have been misidentified as short-lived deep convection. Using Infrared Brightness Temperature (IRBT) from geostationary satellites and TRMM Multisatellite Precipitation Analysis (TMPA) data set, they indicated that the 24-hr future intensity change of TC in the western North Pacific is more closely related to deep convective clouds (DCC, defined as IRBT < 208 K) than the overall precipitation. Several studies have also used the IRBT from geostationary satellites to investigate the overshooting tops (OTs) in TC. Griffin (2017) demonstrated that OTs can aid in characterizing convections within a TC, whereas Monette et al. (2012) showed that OT can be used to predict RI. Sun et al. (2021) also indicated that OT presence is greater in TCs that are rapidly intensifying as compared to those that are undergoing slower intensifications.

By subdividing RI into initial (RI-I, period within 0–12 hr after RI onset) and continuous (RI-C, period within 12–24 hr after RI onset) categories, Zagrodnik and Jiang (2014), Tao and Jiang (2015), and Tao et al. (2017) demonstrated that rainfall, convection, and latent heat distributions differ in the substages of rapidly intensifying TCs. They found that latent heat is stronger during RI-C, and that the area of maximum heating is located closer to the storm center during RI-C than during RI-I (Zagrodnik & Jiang, 2014). Additionally, rainfall frequency (defined by the shear-relative occurrence of near-surface reflectivity greater than 20 dBZ from TRMM PR) in RI-C is also significantly higher than that in RI-I. Although deep convection is concentrated near or within the radius of maximum wind (RMW) during RI, its frequency is significantly higher during RI-C than during RI-I (Tao & Jiang, 2015). This suggests that the abundance of deep convection increases as the storm intensity evolves from RI-I to RI-C.

Cloud properties, such as cloud effective radius (r_e) might indicate the strength of a convective updraft, whereas optical thickness (τ) is closely related to cloud water path, which in ice phase can serve as a proxy of latent heat release during convection (Cecil & Zipser, 1999; Senf & Deneke, 2017). Information on these parameters can be retrieved from instruments onboard polar-orbiting meteorological satellites, such as the Moderate Resolution Imaging Spectroradiometer (MODIS) on Aqua and Terra and Cloud Profiling Radar (CPR) on CloudSat. Directly measuring the cloud microphysical properties is the most preferred method as it would provide detailed information of the cloud microphysical processes. However, data from such method are difficult to obtain for most researchers due to flight safety issue. Cloud top properties from meteorological satellite instruments such as MODIS, are readily available and may still provide invaluable information about some microphysical and radiative properties of clouds. Given the rarity of RI cases, obtaining concurrent and collocated cloud microphysical information from polar orbiting satellites adds to the challenge. The advent of geostationary satellites such as

Japanese Himawari-8 can overcome this difficulty by providing cloud information at a high temporal resolution. Cloud information retrieval from Advanced Himawari Imager (AHI), the primary instrument of Himawari-8, was found to be consistent with that from MODIS and other spaceborne active sensors, including Cloud-Aerosol Lidar with Orthogonal Polarization, CPR onboard Cloud-Aerosol LIDAR and Infrared Pathfinder Satellite Observations, and CloudSat satellites (Liu et al., 2020). The cloud top temperature and cloud top altitudes had been validated against with radiosondes over the South China Sea, with a difference of 1 K and 170 m, respectively.

Cloud and rain characteristics can be investigated by using IRBT and cloud properties obtained from Himawari-8's AHI observations and precipitation from Integrated Multi-satellitE Retrievals for Global Precipitation Measurement (GPM IMERG). Given the inconsistent findings regarding whether DCC or precipitation is a good predictor of RI or not, and the seemingly different characteristics of RI at its initial and continuing stage, this paper aims to investigate the DCC, precipitation, and cloud properties characteristics of rapidly intensifying TCs in the western North Pacific. Specifically, it seeks to answer the following questions: (a) Can DCC or precipitation indicate that RI is underway? If so, what are the possible restrictions of such indicators? (b) Are the deep convection, precipitation, and cloud properties characteristics during RI-I and RI-C really indicative of the onset and continuing stages of RI? Or are they just artifacts of intensity when TC rapidly intensified? Mean and radial distributions of DCC percentage and temperature, precipitation, and cloud properties within 6 RMW of the TC center for various intensity stages and intensification categories are analyzed. The same analysis is done to compare RI-I and RI-C with TCs undergoing RI at different intensity stages. The rest of the paper is arranged as follows. Data and methods are described in Section 2. Results are presented in Section 3. Summary is given in Section 4.

2. Data and Methods

TC position (latitude and longitude), wind speed, and RMW are obtained from International Best Track Archive for Climate Stewardship (Knapp et al., 2010, 2018). Using the maximum wind speed (V_{max}), TCs are classified into intensity stages as follows: $V_{max} \leq 32$ kt (tropical depression or TD), 33 kt $\leq V_{max} \leq 64$ kt (tropical storm or TS), 65 kt $\leq V_{max} \leq 95$ kt (categories 1 and 2 or minor TC), and $V_{max} \geq 96$ kt (categories 3, 4, and 5 or major TC). Using the 24 hr future intensity change ($\Delta V_{max} = V_{max\_t24} - V_{max\_t0}$; where V_{max_t0} is the current intensity and V_{max_t24} is the subsequent 24 hr intensity), TCs are arranged into intensification categories, namely $\Delta V_{max} < 0$ kt (weakening or W), 0 kt $\leq \Delta V_{max} \leq 10$ kt (intensifying neutral or IN), 11 kt $\leq \Delta V_{max} \leq 29$ kt (slow intensification or SI), and $\Delta V_{max} \geq 30$ kt (RI). We utilized 56 TCs that reached category 2 hurricane and underwent RI, in the western North Pacific (study area: 6–37°N latitude and 107–165°E longitude) from January 2016 to September 2021.

IRBT and cloud properties (i.e., r_e, τ, and cloud top height [CTH]) are derived from AHI, with a spatial resolution of 5 × 5 km. Liu et al. (2020) studied the retrieval of cloud microphysical and optical properties from AHI observation. Their results suggested that uncertainties in the cloud top temperature and altitude retrievals agree well with collocated reference data, with low differences of 1 K and 170 m, respectively. Additionally, r_e obtained from AHI are comparable with those from MODIS (Letu et al., 2019; Liu et al., 2020). Following the method of Chen and Houze (1997), and Wu and Ruan (2016), the IRBT threshold value of 208 K is chosen to identify DCC.

Precipitation is obtained from IMERG V06B (Huffman et al., 2019). Specifically, the variable "precipitationCal" or the calibrated precipitation field in 3IMERGHH product is used in this study. Final run is utilized for all TCs. 3IMERGHH have a spatial resolution of 0.1° (10 km, gridded), which we regridded (array is resized using linear interpolation) to 5 km to match the IRBT and cloud data's resolution. In this study, rain is classified using the Philippine Atmospheric, Geophysical and Astronomical Services Administration rain rate (RR) classification as follows: $RR < 0.01$ mm hr^{-1} (no rain), $0.01 \leq RR < 2.5$ mm hr^{-1} (light), $2.5 \leq RR < 7.5$ mm hr^{-1} (moderate), $7.5 \leq RR < 15$ mm hr^{-1} (heavy), $15 \leq RR < 30$ mm hr^{-1} (intense), $RR \geq 30$ mm hr^{-1} (torrential). High temporal and spatial resolutions of IMERG precipitation are important for studying the TC precipitation structure and evolution. However, comparison analysis of IMERG rainfall and gridded hourly rain-gauge data indicates an underestimate of the total TC precipitation (Huang et al., 2021). Despite underestimating the rain intensity, IMERG can depict the phase evolution of the inter-annual variation of rainfall associated with TC (Huang et al., 2021). In this study, rainfall characteristics are mainly described in a qualitative manner as to depict the main features and not the exact quantitative precipitation values.

Table 1
Statistics of Tropical Cyclone for Different Intensity and Intensification Categories, and Rapid Intensification Sub-Categories

Intensity	Intensification	Mean V_{max} (kt)	Mean ΔV_{max} (kt)	Mean RMW (NM)	Sample size: Number of data points [**number of satellite scans/images**]				
					DCC percentage	DCC count	r_e	τ, CTH	Precipitation
TD	W	27	−23	33	2,343,672 [**156**]	115,285 [**156**]	1,492,246 [**156**]	2,065,102 [**156**]	730,821 [**42**]
	IN	21	5	55	8,299,620 [**180**]	483,869 [**180**]	3,716,642 [**168**]	6,096,532 [**168**]	4,982,110 [**105**]
	SI	23	20	51	10,196,100 [**264**]	936,272 [**264**]	6,134,079 [**264**]	8,098,159 [**264**]	5,210,761 [**154**]
	RI	28	36	34	660,675 [**46**]	71,202 [**46**]	451,324 [**46**]	574,507 [**46**]	258,525 [**18**]
TS	W	44	−25	37	6,513,012 [**288**]	222,137 [**288**]	4,490,127 [**288**]	5,655,035 [**288**]	3,799,257 [**168**]
	IN	45	5	47	8,010,216 [**204**]	743,162 [**204**]	5,010,494 [**204**]	6,716,430 [**204**]	4,673,172 [**119**]
	SI	46	21	36	5,174,145 [**323**]	1,001,063 [**323**]	5,937,188 [**454**]	7,668,332 [**454**]	3,754,795 [**195**]
	RI	48	43	31	3,816,096 [**240**]	740,847 [**240**]	2,675,663 [**240**]	3,431,060 [**240**]	2,232,195 [**140**]
Minor TC	W	81	−31	20	4,397,908 [**609**]	892,220 [**609**]	3,377,486 [**609**]	4,131,212 [**609**]	2,026,405 [**300**]
	IN	86	6	19	665,856 [**120**]	166,433 [**120**]	511,978 [**115**]	632,721 [**115**]	249,696 [**45**]
	SI	74	21	20	1,279,596 [**228**]	483,078 [**228**]	988,896 [**227**]	1,237,622 [**227**]	654,689 [**119**]
	RI	80	43	18	1,729,384 [**322**]	681,621 [**322**]	673,464 [**168**]	841,095 [**168**]	502,292 [**98**]
Major TC	W	117	−28	15	1,200,524 [**371**]	552,599 [**371**]	860,160 [**371**]	1,177,424 [**371**]	702,639 [**217**]
	IN	127	5	16	528,924 [**120**]	256,683 [**120**]	326,662 [**119**]	495,508 [**119**]	308,539 [**70**]
	SI	116	19	9	180,716 [**143**]	143,418 [**143**]	86,782 [**143**]	167,614 [**143**]	94,670 [**84**]
	RI	110	36	9	132,434 [**115**]	109,303 [**115**]	61,999 [**115**]	129,216 [**115**]	51,822 [**45**]
TS	RI-I	50	35	32	2,293,104 [**156**]	378,298 [**156**]	1,497,061 [**156**]	1,926,659 [**156**]	955,460 [**65**]
Minor TC	RI-C	90	45	15	600,024 [**156**]	282,240 [**156**]	432,814 [**156**]	579,916 [**156**]	250,010 [**65**]
Total					58,022,006 [**4,041**]	8,259,730 [**4,041**]	38,725,065 [**3,999**]	51,624,144 [**3,999**]	31,437,858 [**2,049**]

RI is sub-categorized into initial and continuing. In this study, the period within 0–3 hr after RI onset is considered as initial RI (RI-I) while the period within 24–27 hr after RI onset is marked as continuing RI (RI-C). It must be noted that for RI-C, the TC has been continuously rapidly intensifying for at least 24 hr. Only daytime (10:00–14:00 local solar time in the study area) IRBT, precipitation, and cloud properties (r_e, τ, and CTH) data are included in this study. Overall, we collected 4041 and 3999 Himawari satellite scans for IRBT and cloud properties, respectively. For precipitation, we used 2049 3IMERGHH products. Based on the radial distribution of DCC percentage and precipitation of TD, we limit our analyses within six times the RMW. This chosen radius is also consistent with radial distance used by Sun et al. (2021).

Table 1 summarizes the mean V_{max}, the mean ΔV_{max}, the mean RMW, sample size, and the number of satellite scans of the TCs at different intensity stages and intensification categories, as well as at RI sub-categories. The sample size corresponds to the total number of data points (and number of satellite scans or images) that were utilized for each variable for a particular combination of intensity stage and intensification category (e.g., TD W, TD IN, TD SI, TD RI, TS W, etc.). Data used in RI sub-categories are independent from the data used in TD RI, TS RI, minor TC RI, and major TC RI. For any intensity stage (except for TD), rapidly intensifying TC (RI TC) has the smallest RMW. This is in agreement with the previous finding—that is, the smaller the RMW is, the more likely the TC is to undergo RI (Carrasco et al., 2014).

3. Results

3.1. Mean DCC, Precipitation, and Cloud Properties

Figure 1 shows the mean DCC percentage (DCC-P) and temperature (DCC-T), precipitation, r_e, τ, and CTH of TC, at various intensity stages and intensification categories, within 6RMW of the TC center. Strong TCs (i.e., minor and major TCs) have higher DCC-P than weak TCs (i.e., TD and TS) regardless of intensification (Figure 1a). Due to their larger RMW (Table 1), the total DCC count per satellite scan within 6 RMW is higher in

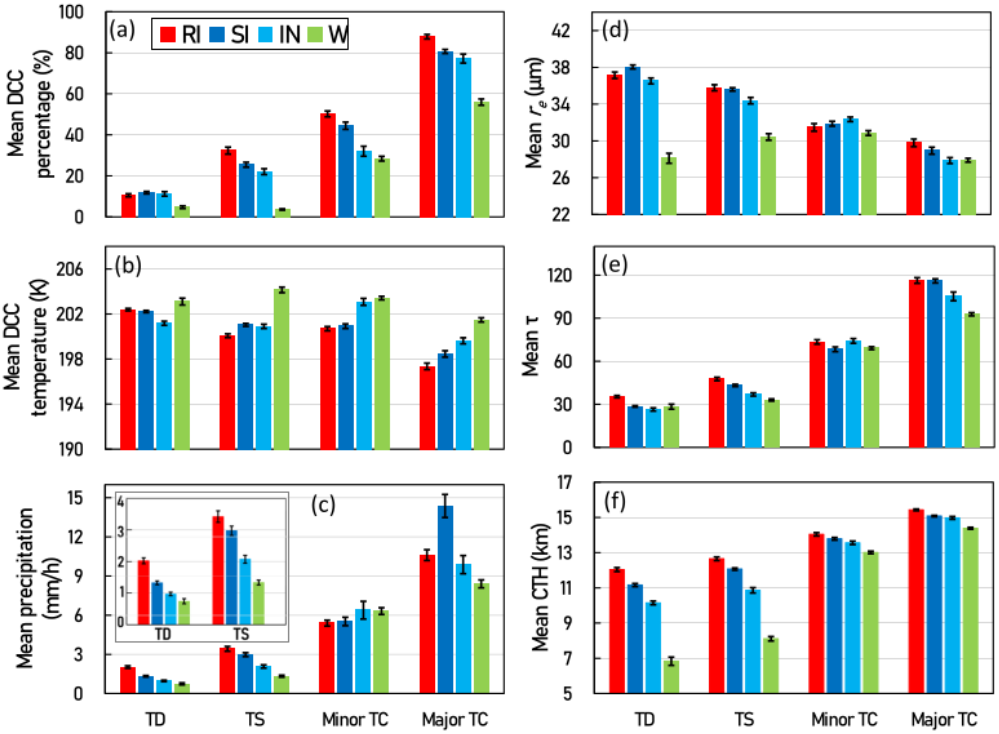

Figure 1. Mean (a) deep convective cloud (DCC) (Infrared Brightness Temperature ≤ 208 K) percentage (DCC-P), (b) DCC temperature (DCC-T), (c) precipitation, (d) cloud effective radius (r_e), (e) cloud optical thickness (τ), and (f) cloud top height (CTH) as a function of tropical cyclone (TC) intensity (V_{max}) and intensification (ΔV_{max}). Values are obtained within six times the radius of maximum wind of TC. Intensity stage includes tropical depression (TD, $V_{max} \leq 32$ kt), tropical storm (TS, 33 kt $\leq V_{max} \leq$ 64 kt), minor TC (65 kt $\leq V_{max} \leq$ 95 kt), and major TC ($V_{max} \geq$ 96 kt). Intensification ($\Delta V_{max} = V_{max\_t24} - V_{max\_t0}$) is calculated by subtracting the current intensity (V_{max_t0}) from the subsequent 24 hr intensity (V_{max_t24}). Intensification category includes rapid intensification ($\Delta V_{max} \geq 30$ kt), slow intensification (11 $\leq \Delta V_{max} \leq$ 29 kt), intensifying neutral (0 $\leq \Delta V_{max} \leq$ 10 kt), and weakening ($\Delta V_{max} < 0$ kt). The inset in panel (c) is the mean precipitation (mm/hr) in TS and TD. Error bars are based on standard error.

weak TCs (~2,500 DCC per satellite scan) than in strong TCs (~16,00 DCC per satellite scan), whereas the area within 6 RMW in weak TCs is ~6.7 times wider than in strong TCs. Hence, the DCC-P in weak TCs is still lower than in strong TCs. This result is consistent with the findings in the study of Sun et al. (2021) which indicated that the OT density (OTD, defined as OT count in a satellite scan per 10,000 km^2) in TS is less than in strong TCs. Moreover, RI TCs (except TD) have the highest percentage of DCC and the coldest mean DCC-T as compared to TCs that are undergoing other intensification (i.e., SI, IN, and W) (Figure 1b). This result is consistent with the study of Ruan and Wu (2018), which showed that RI follow the occurrence of widest coverage of DCC with lowest temperature when compared to other intensification categories.

Mean precipitation is increasing with TC intensity regardless of intensification (Figure 1c). In weak TCs, the mean precipitation has a clear relationship with intensification as RI TCs have the highest mean precipitation as compared to other intensification categories. It should be noted, however, that the precipitation in rapidly intensifying TD and TS are generally light to moderate (Figure 1c inset). On the other hand, highest mean precipitation rate in minor and major TCs is found in IN and SI categories, respectively. Ruan and Wu (2018) showed that precipitation increases with TC intensity. However, they were unable to establish the relationship between precipitation and TC intensification. By contrast, Tao et al. (2017) indicated the importance of wide areal coverage of stratiform rain at the onset of RI, during which the TC is generally in TS category (a weak TC). Ruan and Wu (2018) analyzed the precipitation and the TC intensification, without simultaneously considering the TC intensity, which might weaken the link between RI and precipitation in a particular TC intensity. In this study, the distribution of precipitation is obtained by taking into account both the intensity and intensification at the same time. Consistent with the finding of Tao et al. (2017), our result suggests that the mean precipitation (light to

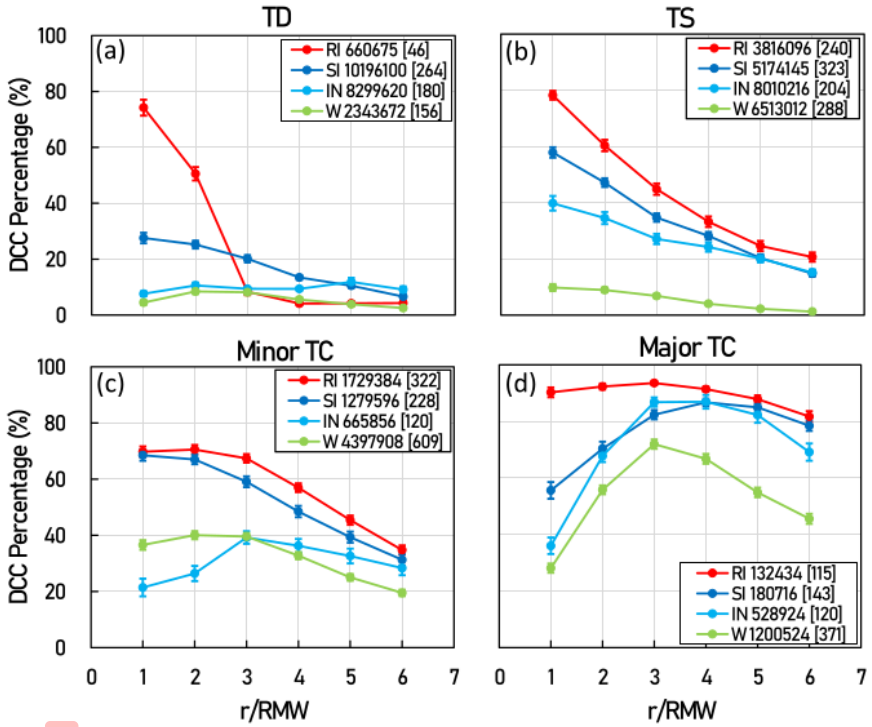

Figure 2. Deep convective clouds-P as a function of radius of maximum wind-normalized radius for tropical cyclone (TC) intensity stage (a) tropical depression, (b) tropical storm, (c) minor TC, and (d) major TC, and intensification category rapid intensification (red), slow intensification (dark blue), intensifying neutral (turquoise), and W (green). The number in the legend represents the number of data points used and inside the bracket is the number of satellite scans. Error bars are based on standard error.

moderate rain) can be indicative of RI in weak TCs. In strong TCs, similar to the finding of Ruan and Wu (2018), the mean precipitation has no clear connection with the TC intensification.

Clouds in strong TCs are comprised of smaller particles, are optically thicker, and have higher CTH than in weak TCs (Figures 1d–1f). In general, RI TCs have the highest τ and CTH as compared to TCs undergoing other intensification (Figures 1e and 1f). However, r_e has an ambiguous relationship with intensification. On the other hand, the CTH, especially in weak TCs, has a clear relationship with intensification. In combination with the results for the mean precipitation (Figure 1c), these suggest a relatively more active role of rain and clouds that reach greater heights, in the RI of weak TCs.

Overall, the mean precipitation and CTH in weak TCs, and the mean DCC-P and DCC-T in strong TCs, have clear relationship with TC intensification and can potentially discriminate RI from other intensification categories.

3.2. Radial Distributions

3.2.1. DCC Percentage and Temperature

The radial distribution of the DCC-P at various TC intensity stages and intensification categories is shown in Figure 2. In rapidly intensifying TD (RI TD), the DCC-P is almost zero at 3–6 RMW but swiftly increased with the decreasing radius within 2 RMW of the TC center (Figure 2a). On the other hand, the DCC-P slightly increased with the decreasing radius in slowly intensifying TD, whereas it is almost constant within 6 RMW in IN and W TD. These results are consistent with the findings of Rogers et al. (2013), which indicated that convective bursts have higher percentage within 1–2 RMW in intensifying as compared to steady state TCs.

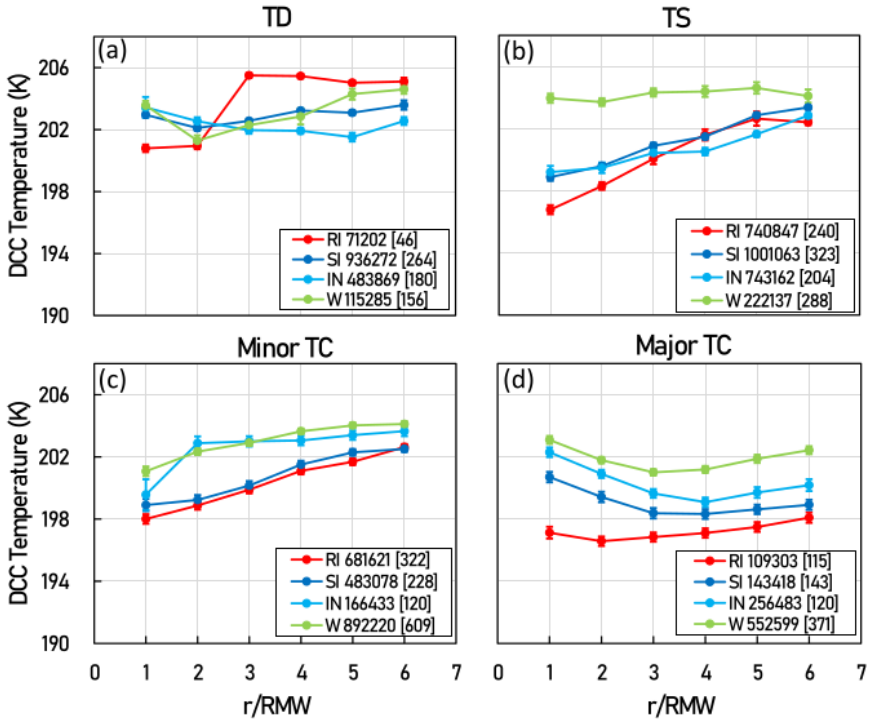

Figure 3. As Figure 2 but for the deep convective clouds-T.

The radial profile of the DCC-P in TS shows that the DCC-P is increasing with the decreasing radius (Figure 2b). Additionally, TS with faster intensification has greater DCC-P and the difference is more remarkable nearer to the storm's center. These results are almost identical with the findings of Sun et al. (2021) regarding the OTD in TS.

In minor TC, the DCC-P is increasing with decreasing radius (except in IN) (Figure 2c). Moreover, the DCC-P in SI and RI are always greater than in IN and W. Similar to that in TS, the difference is more notable closer to the TC center.

In major TC, the DCC-P is lower within 1 RMW then it increased and reached maximum between 3 (RI, IN, and W) and 4 RMW (SI) (Figure 2d). The reduced DCC-P at 1–2 RMW can be attributed to the strong warm core in major TCs, which discourages the growth of deep convection near the center of the storm (Chen & Zhang, 2013). Nonetheless, this feature is not obvious in RI, in which the DCC-P is always greater than 80% at any radial distance within 6 RMW. There are two possible explanations for this feature; (a) It has been known that the strength of warm core increases with TC intensity (Komaromi & Doyle, 2017). The mean V_{max} in RI (110) is less than in SI (116), IN (127), and W (117 kt). The weaker V_{max} in RI can be associated with relatively weaker warm core which might not suppressed the development of convection as strongly as that in SI, IN, and W. For the same reason, the steepest slope in DCC-P is found in IN, the major TC with the strongest V_{max}. (b) Miller et al. (2015) indicated that the formation of more convective bursts within RMW, supported by latent heat of fusion, aided in the RI of a strong TC. The presence of high DCC-P within 1 RMW might be one of features of major TCs that help them rapidly intensify.

The radial distribution of DCC-T in Figure 3 shows that the temperature is generally low when the DCC-P is high (Figure 2). This means that a greater concentration of DCC is mainly of colder temperature. In comparison to the other intensification categories, RI has lowest DCC-T within 2 RMW for weak TCs (Figures 3a and 3b) and within at least 5 RMW for strong TCs (Figures 3c and 3d). In combination with the radial distribution of DCC for different TC intensity stages and intensification categories in Figure 2, this indicates that the highest percentage and lowest temperature of DCC found in RI TC, within 2 RMW in weak TCs, and within 5 RMW in strong TCs,

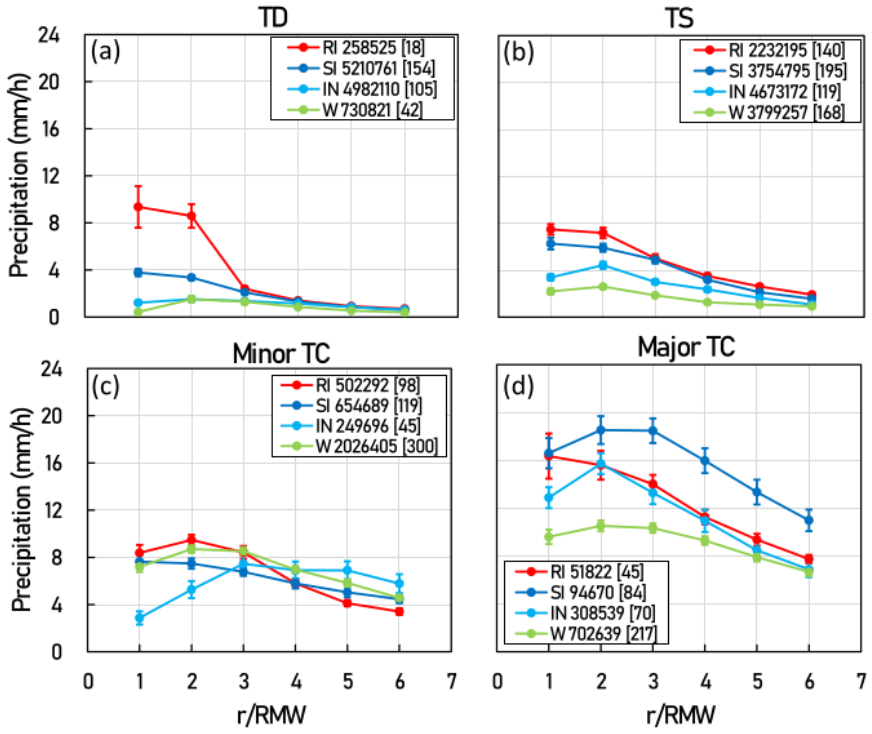

Figure 4. As Figure 2 but for the precipitation.

can potentially differentiate RI from other intensification categories. Moreover, it is worth noting that in major TC, the DCC-T is arranged from coldest to warmest with decreasing intensification (RI, SI, IN, and W, respectively) (Figure 3d). This suggests that in major TCs, when a storm generally has more concentric pattern of deep convection (S. Yang et al., 2020), the DCC-T alone may be used to determine the onset of RI.

While the mean DCC-P and DCC-T in TD are unable to present a clear distinction between the intensification categories (Figure 1a), the radial profiles indicate that within 2 RMW, the DCC-P and DCC-T categorically discriminate RI from non-rapidly intensifying (non-RI) TD (Figures 2a and 3a). In storms stronger than TD, the mean DCC-P and DCC-T clearly differentiated the TC intensifications (Figure 1a). Furthermore, their radial distributions of the DCC-P, anywhere within 6 RMW, is always greater in RI than other intensification categories (Figures 2b–2d). Whereas, the radial distribution of the DCC-T in hurricanes, especially in major TCs, provides an additional and clear delineation between the intensifications (Figures 3b–3d).

3.2.2. Precipitation

Figure 4 shows the radial distribution of precipitation at various TC intensity stages and intensification categories. In general, weak TCs have lower precipitation than strong TCs, anywhere within 6 RMW. Apart from having larger RMW, weak TCs also have less symmetric precipitation structure than strong TCs (S. Yang et al., 2021) which may have led to their lower mean precipitation. The precipitation within 2 RMW of RI TC is always higher than non-RI TC, except in major TC. In weak TCs, the precipitation rate within 2 RMW is sorted according to intensification–that is, the stronger the intensification is, the higher the precipitation (Figures 4a and 4b). This is not observed in strong TCs, however (Figures 4c and 4d).

Several studies have highlighted the importance of shallow convection at the onset RI (Kieper & Jiang, 2012; Tao et al., 2017; Zagrodnik & Jiang, 2014). It must be pointed out that in their studies, most of the TCs are in TS category (a weak TC) when the RI commenced. Consistent with their findings, our results show that in weak TCs, the mean precipitation (light to moderate rain) (Figure 1c) clearly reflects the TC intensification. Furthermore,

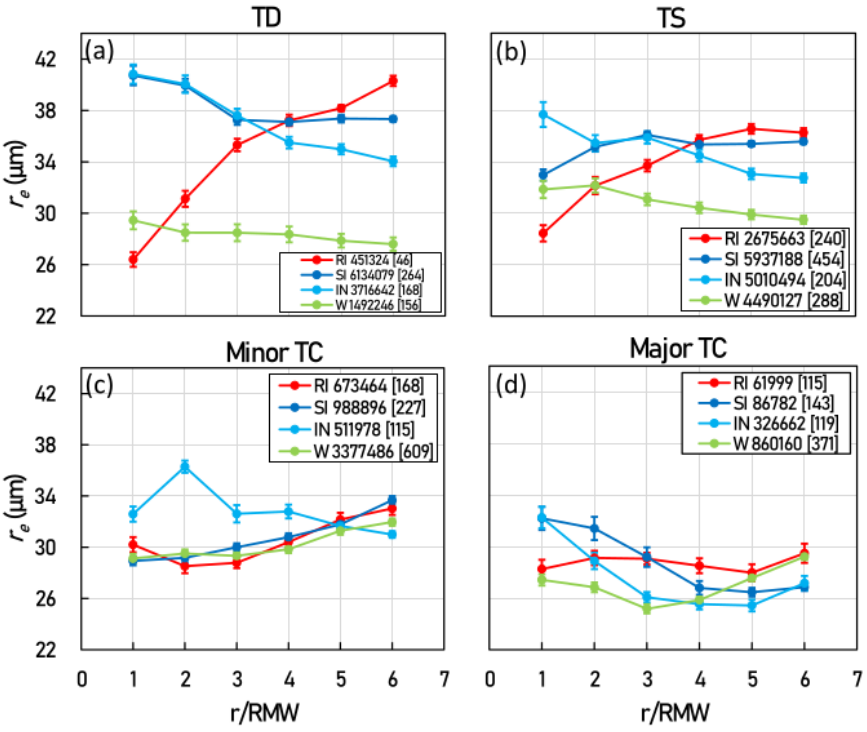

Figure 5. As Figure 2 but for the r_e.

the radial profile further specifies the location, at 2 RMW, in which the precipitation is significantly higher in rapidly intensifying weak TCs than in other intensification categories (Figures 4a and 4b). By contrast, both the mean and radial profile of precipitation do not provide a clear distinction between the intensifications in strong TCs (Figures 1c, 4c, and 4d). This result is consistent with the findings of Ruan and Wu (2018), who indicated that TC intensification is more related to DCC than precipitation. It must be mentioned that in their study, RI TC has a mean V_{max} ~61 kt (standard deviation ~23 kt), which is nearly a category 1 hurricane.

3.2.3. Cloud Properties

Figure 5 shows the radial distribution of the r_e. One of the prominent features in the radial distribution of r_e in rapidly intensifying weak TCs (Figures 5a and 5b) is that the r_e near the storm's center is very much smaller (26–28 μm) as compared to the r_e at 6 RMW (36–40 μm). Mecikalski et al. (2011) showed that cloud top droplets became small as a result of ice glaciation and particle settling with deepened cumuli. The large r_e gradient we observed is likely an indication of considerable difference in the deep convective activities within the 6 RMW in rapidly intensifying weak TCs. In particular, this suggests that in rapidly intensifying weak TCs, the DCCs near the center are mostly in a mature stage of development, whereas the DCCs that are located farther away from the center are mainly in a developing or dissipating stage. This is consistent with the coldest DCC-T and highest precipitation rate we found within the 2 RMW in rapidly intensifying TD and TS (Figures 3a, 3b, 4a, and 4b). In strong TCs, the r_e's radial distribution within 6 RMW suggests that clouds generally prefer a particular particle size (28–34 μm in minor TC; 25–33 μm in major TC). The uniform cloud particle size in strong TCs may be attributed partially to their narrower RMW range (18–20 NM in minor TC; 9–16 NM in major TC) as compared with in weak TCs (34–55 NM in TD; 31–47 NM in TS). Also, major TCs have faster maximum wind speed than minor TCs, which may have likely led to a more homogenous and small r_e.

The radial distribution of τ (Figure 6) shows that τ is mainly influenced by the precipitation (Figure 4), except in major TC. In other words, in TD, TS, and minor TC, the precipitation (Figures 4a–4c) mainly determines the optical thickness of a cloud (Figures 6a–6c), whereas in major TC, the DCC (Figure 2d) generally influences

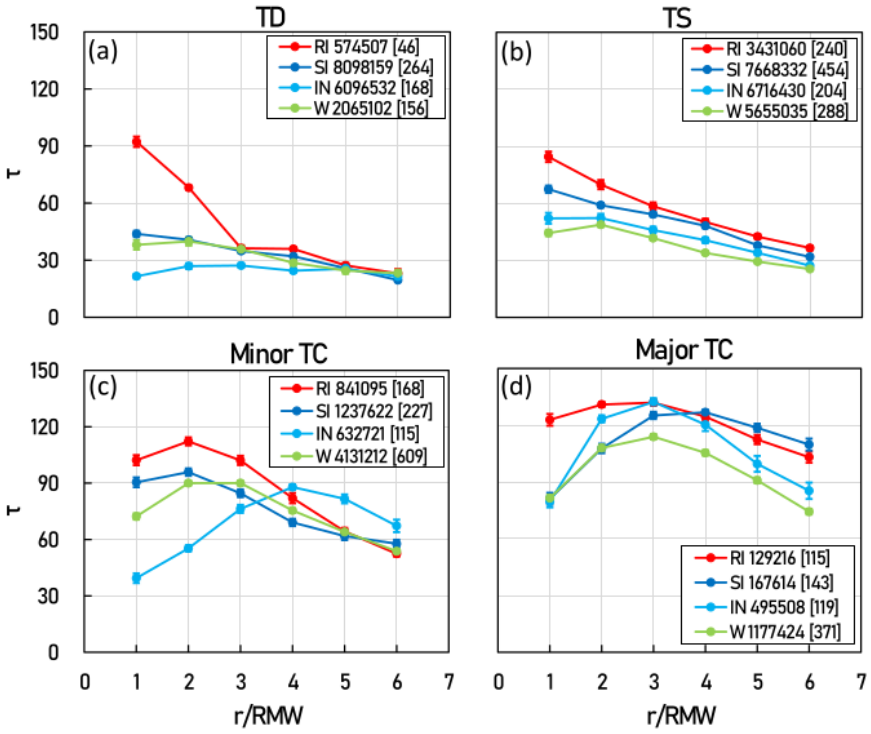

Figure 6. As Figure 2 but for the τ.

the τ (Figure 6d). The optically thickest clouds are found near the storm's center of weak TCs while they are at 2–4 RMW in strong TCs. Similar to the reason provided for in Figure 2d, strong warm core associated with strong TCs may have likely prevented the formation of optically thick clouds near the center of the TCs. In any intensity stage, within at least 2 RMW, the τ is always higher in RI TC than non-RI TC. This suggests the crucial significance of optically thicker clouds near the storm's center in the RI of any TC.

Figure 7 presents the radial distribution of CTH. In general, the CTH is higher in RI TC than in any other intensification categories. In particular, the CTH in TD is arranged in ascending order with increasing intensification (Figure 7a). Thus, the CTH alone then may be used to determine whether a TD is at the onset RI or not.

3.3. Characteristics During Initial and Continuing RI

3.3.1. Mean DCC, Precipitation, and Cloud Properties

Distributions of the mean DCC, precipitation, and cloud properties in RI-I and RI-C as well as in rapidly intensifying TD, TS, minor TC, and major TC are shown in Figure 8. The x-axis in Figure 8 is arranged in descending mean RMW as follows: RI TD (34 NM), RI-I (32 NM), RI TS (31 NM), RI minor TC (18 NM), RI-C (15 NM), and RI major TC (9 NM) (Table 1). It can be noted that although RI-I is on average a TS, it has slower RI (and larger RMW) than RI TS, while RI-C is on average a minor TC and has faster RI (and smaller RMW) than RI minor TC (Table 1). The mean DCC-P (Figure 8a), precipitation (Figure 8c), τ (Figure 8e), and CTH (Figure 8f) within 6 RMW in RI TCs are increasing with decreasing RMW (or increasing intensity). This follows that RI-C has higher mean DCC-P, precipitation, τ, and CTH than RI-I. In general, the mean DCC-T (Figure 8b) decreases with decreasing RMW while r_e (Figure 8d) is smaller in rapidly intensifying strong TCs (i.e., RI minor TC, RI-C, and RI major TC) than in rapidly intensifying weak TCs (i.e., RI TD, RI-I, and RI TS). As such, the mean DCC-T is lower and r_e is smaller in RI-C than in RI-I. Hence, the above-mentioned characteristics of the mean DCC,

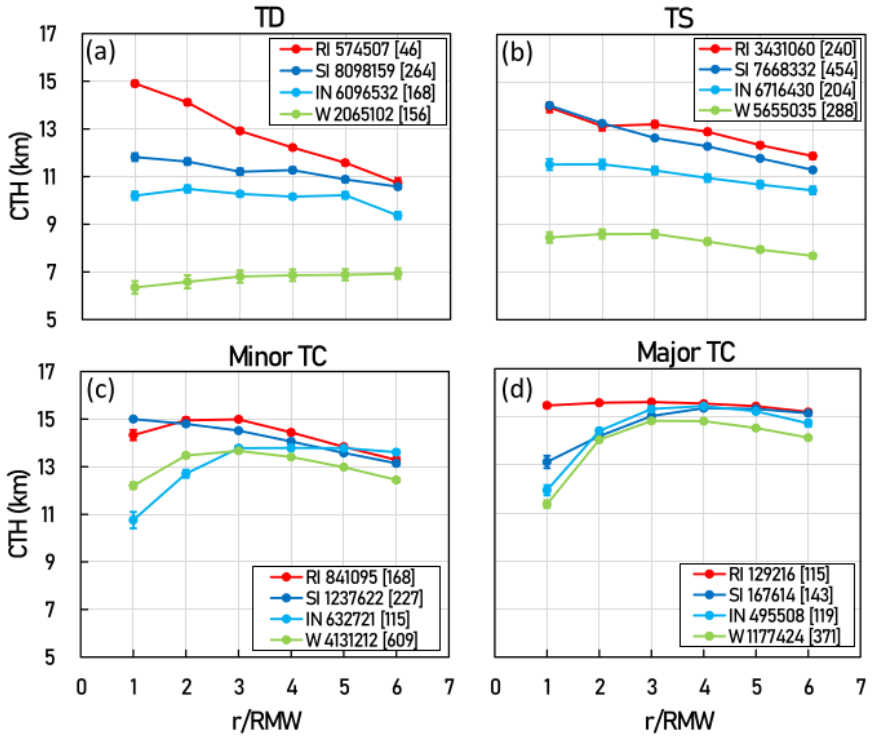

Figure 7. As Figure 2 but for the cloud top height.

precipitation, and cloud properties during the onset and continuing stages of RI are highly indicative of their RMW sizes (or current intensities and RI rates).

3.3.2. Radial Distributions of DCC, Precipitation, and Cloud Properties

The radial profiles of DCC-P and DCC-T are shown in Figures 9a and 9b. In general, higher concentration, and colder DCC is found in RI TC with stronger intensity. Near the center of RI TCs, clouds are at least 70% deep convective and have the coldest temperatures (in RI TD ~201 K, in all RI TCs except RI TD ~196–198 K). With an increasing distance from the storm's center, the DCC-P is decreasing and temperature is increasing in a manner that manifests their RMW sizes. Steeper decrease in DCC concentration and more drastic increase of DCC-T occur in TCs with larger RMW (rapidly intensifying weak TCs) than with smaller RMW (rapidly intensifying strong TCs). Several studies had emphasized the significance of deep convection near the center in the RI of a TC. Lin et al. (2021) indicated that the abundance of deep convection near the center of Hagibis (2019), and in a ring surrounding the center collocated with RMW of Haiyan (2013) more likely contributed to their RI. Also, Miller et al. (2015) showed that the development of convective bursts within RMW favored the RI of Wilma (2005). Consistent with Lin et al. (2021) and Miller et al. (2015), our result indicates that within 1 RMW of RI TC, clouds are largely deep convective regardless of the intensity of the TC.

The radial distribution of precipitation in RI TCs (except RI TD) demonstrate their current stages—that is, the higher the intensity of a RI TC is, the stronger the precipitation (Figure 9c). Near the storm's center of RI TC, the precipitation is at least in heavy category and it generally decrease outside 2 RMW.

Clouds near the center of RI TC are made of smallest particles (r_e ~26–30 μm) when compared to those at 2–6 RMW (Figure 9d). Within 3 RMW of the TC center, smaller RMW (and high DCC-P) in rapidly intensifying strong TCs led an almost uniform r_e while larger RMW (and sharp decrease of DCC-P) in rapidly intensifying weak TCs cause their r_es to increase drastically (Figures 9a and 9d). Clouds with highest τ and CTH are found

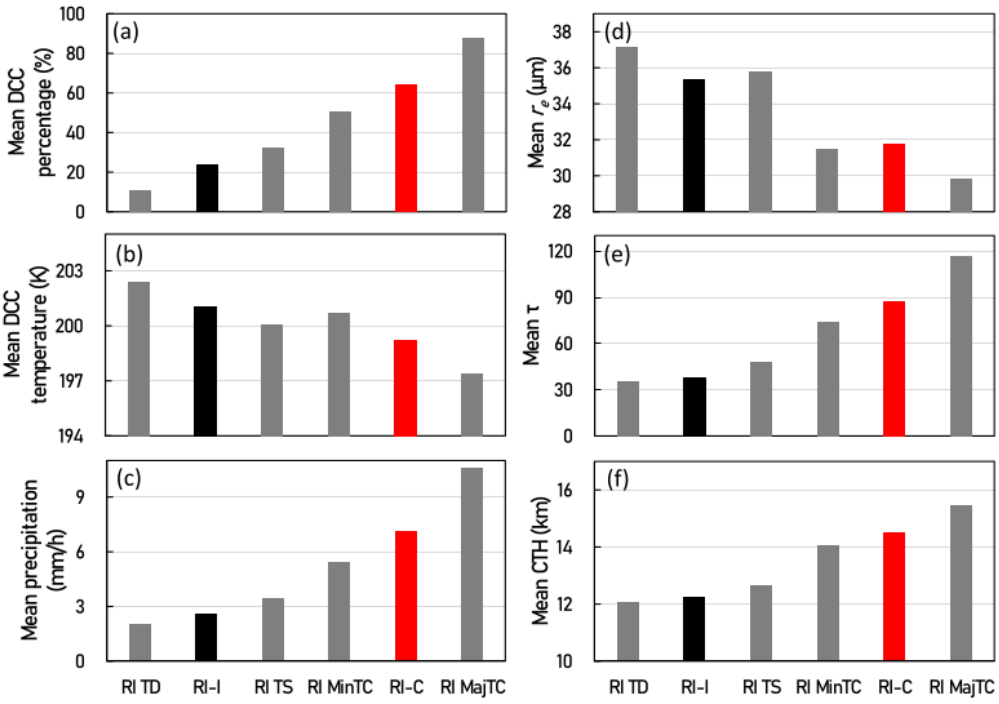

Figure 8. Mean (a) deep convective clouds (DCC)-P, (b) DCC-T, (c) precipitation, (d) r_e, (e) τ, and (f) cloud top height in initial rapid intensification (RI-I, the period within 0–3 hr after RI onset) (black) and continuing RI (RI-C, the period within 24–27 hr after RI onset and the tropical cyclone [TC] has been continuously rapidly intensifying for at least 24 hr) (red) as well as in rapidly intensifying tropical depression, tropical storm, minor TC, and major TC (gray).

near the center of rapidly intensifying weak TCs while they are located at 2–3 RMW in rapidly intensifying strong TCs (Figures 9e and 9f). Near the center of RI TC, the τ is at least ~80 and CTH is at least ~14 km.

The above descriptions of RI TCs provide the bases of the general distinction of the radial profiles of DCC, precipitation, and cloud properties between RI-I and RI-C. Because of its smaller RMW (or higher intensity), the DCC-P, precipitation, τ, and CTH are generally higher in RI-C than in RI-I. For the same reason, the DCC-T is lower and r_e is smaller in RI-C than in RI-I. In other words, within the domain of RI category, the variation in the deep convection, precipitation, and cloud properties that we identified between RI-I and RI-C are likely just due to their different RMW sizes (or TC intensities and RI rates). Thus, the higher rainfall frequency found in RI-C than in RI-I by Zagrodnik and Jiang (2014) may be attributed to the then current intensities of TCs when they underwent RI. Moreover, since TCs during RI-C have faster RI rate than during RI-I, the precipitation peak at 2 RMW in RI-C (Figure 9c) can be attributed to a more symmetric distribution of rain associated with higher intensification rate (Alvey et al., 2015). Also, this peak might be an indication of a precipitation ring that may form as RI TC strengthens (Kieper & Jiang, 2012). Furthermore, since TCs during RI-C have higher intensity than during RI-I, this peak can be a manifestation of concentric pattern of maximum *RR* that is likely to form in stronger storms (S. Yang et al., 2021).

4. Summary

The primary goal of this study is to investigate the DCC, precipitation, and cloud properties (i.e., r_e, τ, and CTH) of RI TCs in the western North Pacific in recent 5 years. Both mean and radial distribution of the variables in various TC intensity stages (TD, TS, minor TC, and major TC) and intensification categories (RI, SI, IN, and W), as well as in initial and continuing RI, are analyzed. The main findings of this study are summarized as follows:

1. The mean DCC-P and DCC-T (within 6 RMW) clearly discriminate the intensifications in TCs stronger than TD (Figures 1a and 1b). Whereas, their radial distributions within 2 RMW in TD (Figure 2a) and at least

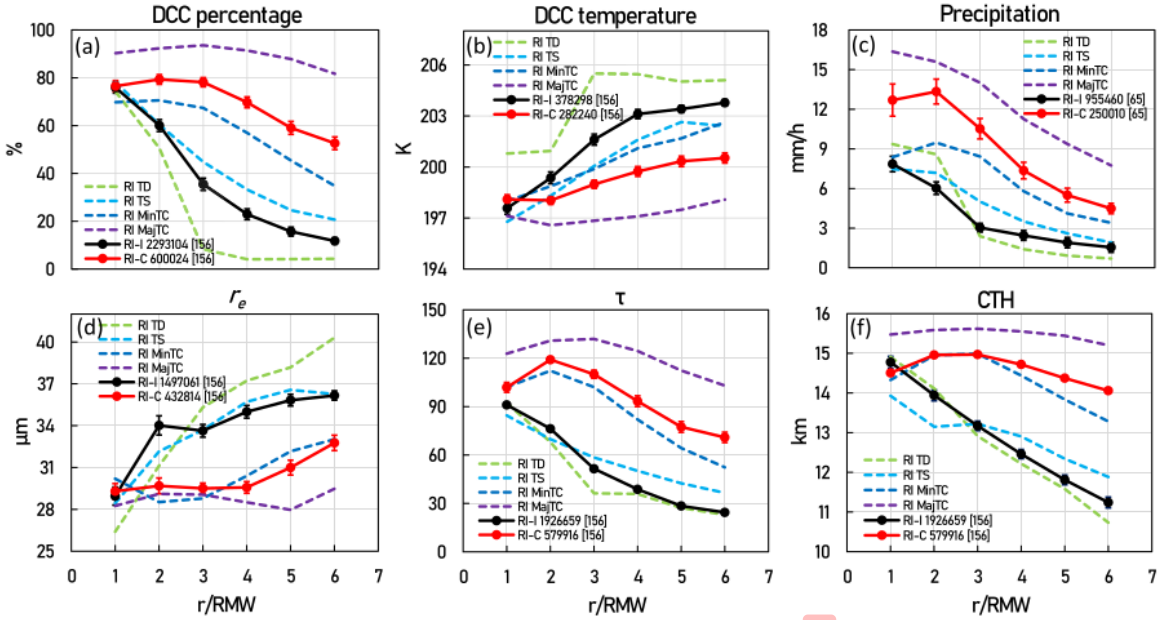

Figure 9. (a) Deep convective clouds (DCC)-P, (b) DCC-T, (c) precipitation, (d) r_e, (e) τ, and (f) cloud top height as a function of radius of maximum wind-normalized radius in rapid intensification (RI)-I (black), and RI-C (red). Error bars are based on standard error. Dashed lines (without markers and standard error bars) are the radial profiles of RI tropical cyclone (TC) at intensity stage tropical depression (green), tropical storm (turquoise), minor TC (dark blue), and major TC (purple). The number in the legend represents the number of data points used and inside the bracket is the number of satellite scans.

within 5 RMW in TCs stronger than TD (Figures 2b–2d), show that RI TC has the highest concentration of coldest DCC as compared to other intensification categories. Additionally, in major TCs, the radial distribution of the DCC-T plainly delineates RI from other intensification categories.

2. In weak TCs (i.e., TD and TS), both the mean (within 6 RMW) and radial distribution (within 2 RMW) of precipitation increases with the TC intensification (Figures 1c, 4a, and 4b). By contrast, the mean and radial profile of precipitation in strong TCs (i.e., minor and major TCs) do not provide a clear distinction between the intensifications (Figures 1c, 4c, and 4d).
3. Based on the mean values, clouds in strong TCs have smaller r_e, higher τ, and higher CTH than in weak TCs (Figures 1d–1f). The radial distribution of r_e indicates that in weak TCs, the cloud particle size varies considerably with the radial distance from the center, while in strong TCs, clouds prefer a uniform particle size (Figure 5). Within 2 RMW, clouds in RI TC have higher τ than non-RI TC regardless of TC intensity stage (Figure 6). Whereas, the radial profile of CTH in weak TCs discriminates RI from non-RI TCs (Figures 7a and 7b).
4. A TC undergoing RI, regardless of its intensity stage, has the following general characteristics near its center: DCC percentage is very high (>70%), DCC-T is frigid (<201 K), precipitation is heavy to torrential (>7.5 mm/hr), r_e is small (26–30 μm), τ is very thick (>80), and CTH is towering (>14 km) (Figure 9).
5. The variations in the characteristics of deep convection, precipitation, and cloud properties between RI-I and RI-C are apparently due to the difference in their RMW sizes (or current intensities and RI rates) (Figures 8 and 9).

The main findings 1 and 2 are consistent with the findings of Ruan and Wu (2018) and Tao et al. (2017), which indicated that DCC (especially its radial distribution) and stratiform rain, respectively, may be used to predict RI. The precipitation that we found in weak TCs are associated mainly with deep convection, especially within 2 RMW. We argue that light to moderate precipitation may still be used as a predictor for RI in weak TCs. The stratiform rain within a TC is generated primarily by convection. The connection between TC intensification and precipitation is clear in weak TCs because the intensification is largely driven by the release of latent heat during the phase transitions in cloud microphysical processes (H. L. Yang et al., 2015). However, this plain relationship

may vanish in minor and major TCs as the intensification at stronger intensities is mainly influenced not only by the release of latent heat but frontogenetical forcings as well (Li et al., 2019). Thus, we find an indiscernible trend in the precipitation of strong TCs at different intensification categories.

The main finding 3 indicates that deep convective activities vary considerably with the radial distance from the center in rapidly intensifying weak TCs. The small r_e, high τ, and high CTH within 2 RMW of rapidly intensifying weak TCs suggest that the cloud near the center has already deepened, whereas the clouds that are located farther away from the center are mainly in a developing or dissipating stage. Reasonably, the highest DCC-P, coldest DCC-T and highest precipitation rate are found within the 2 RMW in rapidly intensifying TD and TS.

The main finding 4 means that RI TCs exhibit common DCC, precipitation, and cloud properties characteristics near the center of the TC. The main finding 5 implies that it is more appropriate to study RI by sub-categorizing them based on their RMW sizes (or current intensities and RI rates) than initial and continuing stages. This is in accordance with the findings of Carrasco et al. (2014) and Lin et al. (2021), which underscored the importance of RMW and radius of 34-kt winds, respectively, in the RI of a TC.

In this study, the classification of a TC is based on its intensity and intensification, as well as whether it is at the onset or 24 hr of RI. Although environmental conditions have limited influence on the rate of TC intensification (Hendricks et al., 2010), classification based on whether or not a TC is embedded in a favorable environment, may help in understanding some characteristics of DCC and precipitation. Lastly, the time window in this study is only 4 hr (10:00–14:00 local solar time), which cannot take into account some TC processes that take longer time such as eyewall replacement cycle. Appropriate time window is suggested to be determined, if aiming to characterize the dynamics of such TC process.

Data Availability Statement

Research product of L1 Gridded Data and L2 Cloud property (produced from Himawari-8) that were used in this paper were supplied by the P-Tree System, Japan Aerospace Exploration Agency (https://www.eorc.jaxa.jp/ptree/) with a registered account. International Best Track Archive for Climate Stewardship data can be downloaded from the NOAA website (https://www.ncdc.noaa.gov/ibtracs/index.php?name=ib-v4-access). GPM IMERG can be download from the NASA ftp site (ftp://arthurhou.pps.eosdis.nasa.gov/gpmdata) also with registered account. Analyzed IRBT, precipitation, and cloud properties data sets for rapidly intensifying tropical cyclones (2016–September 2021) are available at https://doi.org/10.5281/zenodo.7151903 (Punay & Liu, 2022).

Acknowledgments

This work is supported by the Ministry of Science and Technology of Taiwan (Grants MOST 110-2111-M-001-016, MOST 110-2625-M-001-001, MOST 111-2923-M-001-004-MY2, and MOST 111-2111-M-001-010). Jason Pajimola Punay is supported in part by Academia Sinica (Grants AS-TP-107-M10-3 and AS-GC-110-01). Authors would like to acknowledge the help from Mr. Chi-Hao Chiu in the preparation of partial cloud science data.

References

Alvey, G. R., III, Zawislak, J., & Zipser, E. (2015). Precipitation properties observed during tropical cyclone intensity change. *Monthly Weather Review*, *143*(11), 4476–4492. https://doi.org/10.1175/MWR-D-15-0065.1

Carrasco, C. A., Landsea, C. W., & Lin, Y. L. (2014). The influence of tropical cyclone size on its intensification. *Weather and Forecasting*, *29*(3), 582–590. https://doi.org/10.1175/WAF-D-13-00092.1

Cecil, D. J., & Zipser, E. J. (1999). Relationships between tropical cyclone intensity and satellite-based indicators of inner core convection: 85-GHz ice-scattering signature and lightning. *Monthly Weather Review*, *127*(1), 103–123. https://doi.org/10.1175/1520-0493(1999)127<0103:RBTCIA>2.0.CO;2

Chang, C.-C., & Wu, C.-C. (2017). On the processes leading to the rapid intensification of Typhoon Megi (2010). *Journal of the Atmospheric Sciences*, *74*(4), 1169–1200. https://doi.org/10.1175/JAS-D-16-0075.1

Chen, H., & Zhang, D. L. (2013). On the rapid intensification of Hurricane Wilma (2005). Part II: Convective bursts and the upper-level warm core. *Journal of the Atmospheric Sciences*, *70*(1), 146–162. https://doi.org/10.1175/JAS-D-12-062.1

Chen, S. S., & Houze, R. A., Jr. (1997). Diurnal variation and life-cycle of deep convective systems over the tropical Pacific warm pool. *Quarterly Journal of the Royal Meteorological Society*, *123*(538), 357–388. https://doi.org/10.1002/qj.49712353806

Cione, J. J., & Uhlhorn, E. W. (2003). Sea surface temperature variability in hurricanes: Implications with respect to intensity change. *Monthly Weather Review*, *131*(8 PART 2), 1783–1796. https://doi.org/10.1175//2562.1

Črnivec, N., Smith, R. K., & Kilroy, G. (2016). Dependence of tropical cyclone intensification rate on sea-surface temperature. *Quarterly Journal of the Royal Meteorological Society*, *142*(697), 1618–1627. https://doi.org/10.1002/qj.2752

DeMaria, M., Mainelli, M., Shay, L. K., Knaff, J. A., & Kaplan, J. (2005). Further improvements to the statistical hurricane intensity prediction scheme (SHIPS). *Weather and Forecasting*, *20*(4), 531–543. https://doi.org/10.1175/WAF862.1

Griffin, S. (2017). Climatology of tropical overshooting tops in North Atlantic tropical cyclones. *Journal of Applied Meteorology and Climatology*, *56*(6), 1783–1796. https://doi.org/10.1175/JAMC-D-16-0413.1

Hack, J. J., & Schubert, W. H. (1986). Nonlinear response of atmospheric vortices to heating by organized cumulus convection. *Journal of the Atmospheric Sciences*, *43*(15), 1559–1573. https://doi.org/10.1175/1520-0469(1986)043<1559:NROAVT>2.0.CO;2

Hendricks, E. A., Peng, M. S., Fu, B., & Li, T. (2010). Quantifying environmental control on tropical cyclone intensity change. *Monthly Weather Review*, *138*(8), 3243–3271. https://doi.org/10.1175/2010MWR3185.1

Huang, W.-R., Liu, P.-Y., Chang, Y.-H., & Lee, C.-A. (2021). Evaluation of IMERG level-3 products in depicting the July to October rainfall over Taiwan: Typhoon versus non-Typhoon. *Remote Sensing*, *13*(4), 622. https://doi.org/10.3390/rs13040622

Huffman, G. J., Stocker, E. F., Bolvin, D. T., Nelkin, E. J., & Tan, J. (2019). *GPM IMERG final precipitation L3 half hourly 0.1 degree x 0.1 degree V06*. Goddard Earth Sciences Data and Information Services Center (GES DISC). https://doi.org/10.5067/GPM/IMERG/3B-HH/06

Kaplan, J., & DeMaria, M. (2003). Large-scale characteristics of rapidly intensifying tropical cyclones in the North Atlantic basin. *Weather and Forecasting*, *18*(6), 1093–1108. https://doi.org/10.1175/1520-0434(2003)018<1093:LCORIT>2.0.CO;2

Kaplan, J., DeMaria, M., & Knaff, J. A. (2010). A revised tropical cyclone rapid intensification index for the Atlantic and eastern North Pacific basins. *Weather and Forecasting*, *25*(1), 220–241. https://doi.org/10.1175/2009WAF2222280.1

Kieper, M. E., & Jiang, H. (2012). Predicting tropical cyclone rapid intensification using the 37 GHz ring pattern identified from passive microwave measurements. *Geophysical Research Letters*, *39*(13), L13804. https://doi.org/10.1029/2012GL052115

Knapp, K. R., Diamond, H. J., Kossin, J. P., Kruk, M. C., & Schreck, C. J. (2018). *International best track archive for climate stewardship (IBTrACS) project, version 4. WP*. NOAA National Centers for Environmental Information. https://doi.org/10.25921/82ty-9e16.09.27.2021

Knapp, K. R., Kruk, M. C., Levinson, M. C., Diamond, H. J., & Neumann, C. J. (2010). The international best track archive for climate stewardship (IBTrACS): Unifying tropical cyclone best track data. *Bulletin of the American Meteorological Society*, *91*(3), 363–376. https://doi.org/10.1175/2009BAMS2755.1

Komaromi, W. A., & Doyle, J. D. (2017). Tropical cyclone outflow and warm core structure as revealed by HS3 dropsonde data. *Monthly Weather Review*, *145*(4), 1339–1359. https://doi.org/10.1175/MWR-D-16-0172.1

Letu, H., Nagao, T. M., Nakajima, T. Y., Riedi, J., Ishimoto, H., Baran, A. J., et al. (2019). Ice cloud properties from Himawari-8/AHI next-generation geostationary satellite: Capability of the AHI to monitor the DC cloud generation process. *IEEE Transactions on Geoscience and Remote Sensing*, *57*(6), 3229–3239. https://doi.org/10.1109/TGRS.2018.2882803

Li, M. X., Ping, F., Tang, X. B., & Yang, S. (2019). Effects of microphysical processes on the rapid intensification of Super-Typhoon Meranti. *Atmospheric Research*, *219*, 77–94. https://doi.org/10.1016/j.atmosres.2018.12.031

Lin, I.-I., Rogers, R. F., Huang, H.-C., Liao, Y.-C., Herndon, D., Yu, J.-Y., et al. (2021). A tale of two rapidly-intensifying supertyphoons: Hagibis (2019) and Haiyan (2013). *Bulletin of the American Meteorological Society*, *102*(9), 1–59. https://doi.org/10.1175/bams-d-20-0223.1

Liu, C.-Y., Chiu, C.-H., Lin, P.-H., & Min, M. (2020). Comparison of cloud-top property retrievals from advanced Himawari imager, MODIS, CloudSat/CPR, CALIPSO/CALIOP, and radiosonde. *Journal of Geophysical Research: Atmospheres*, *125*(15), e2020JD032683. https://doi.org/10.1029/2020JD032683

Mainelli, M. M., DeMaria, M., Shay, L. K., & Goni, G. (2008). Application of oceanic heat content estimation to operational forecasting of recent Atlantic category 5 hurricanes. *Weather and Forecasting*, *23*(1), 3–16. https://doi.org/10.1175/2007WAF2006111.1

Mecikalski, J. R., Watts, P. D., & Koenig, M. (2011). Use of Meteosat Second Generation optimal cloud analysis fields for understanding physical attributes of growing cumulus clouds. *Atmospheric Research*, *102*(1–2), 175–190. https://doi.org/10.1016/j.atmosres.2011.06.023

Miller, W., Chen, H., & Zhang, D. L. (2015). On the intensification of Hurricane Wilma (2005). Part III: Effects of latent heat of fusion. *Journal of the Atmospheric Sciences*, *72*(10), 3829–3849. https://doi.org/10.1175/JAS-D-14-0386.1

Monette, S. A., Velden, C. S., Griffin, K. S., & Rozoff, C. M. (2012). Examining trends in satellite-detected tropical overshooting tops as a potential predictor of tropical cyclone rapid intensification. *Journal of Applied Meteorology and Climatology*, *51*(11), 1917–1930. https://doi.org/10.1175/JAMC-D-11-0230.1

Nguyen, L. T., & Molinari, J. (2012). Rapid intensification of a sheared, fast-moving hurricane over the gulf stream. *Monthly Weather Review*, *140*(10), 3361–3378. https://doi.org/10.1175/MWR-D-11-00293.1

Nolan, D. S., Moon, Y., & Stern, D. P. (2007). Tropical cyclone intensification from asymmetric convection: Energetics and efficiency. *Journal of the Atmospheric Sciences*, *64*(10), 3377–3405. https://doi.org/10.1175/JAS3988.1

Pun, I.-F., Chan, J. C. L., Lin, I.-I., Chan, K. T. F., Price, J. F., Ko, D. S., et al. (2019). Rapid intensification of Typhoon Hato (2017) over shallow water. *Sustainability*, *11*(13), 3709. https://doi.org/10.3390/su11133709

Pun, I.-F., Lin, I.-I., & Lo, M. H. (2013). Recent increase in high tropical cyclone heat potential area in the Western North Pacific Ocean. *Geophysical Research Letters*, *40*(17), 4680–4684. https://doi.org/10.1002/grl.50548

Punay, J. P., & Liu, C.-Y. (2022). Analysed data set for rapidly intensifying tropical cyclones in the western North Pacific [Dataset]. Zenodo. https://doi.org/10.5281/zenodo.7151904

Rogers, R., Reasor, P., & Lorsolo, S. (2013). Airborne Doppler observations of the inner-core structural differences between intensifying and steady-state tropical cyclones. *Monthly Weather Review*, *141*(9), 2970–2991. https://doi.org/10.1175/MWR-D-12-00357.1

Ruan, Z., & Wu, Q. (2018). Precipitation, convective clouds, and their connections with tropical cyclone intensity and intensity change. *Geophysical Research Letters*, *45*(2), 1098–1105. https://doi.org/10.1002/2017GL076611

Senf, F., & Deneke, H. (2017). Satellite-based characterization of convective growth and glaciation and its relationship to precipitation formation over central Europe. *Journal of Applied Meteorology and Climatology*, *56*(7), 1827–1845. https://doi.org/10.1175/JAMC-D-16-0293.1

Shu, S., Zhang, F., Ming, J., & Wang, Y. (2014). Environmental influences on the intensity changes of tropical cyclones over the western North Pacific. *Atmospheric Chemistry and Physics*, *14*(12), 6329–6342. https://doi.org/10.5194/acp-14-6329-2014

Simpson, J., Halverson, J. B., Ferrier, B. S., Petersen, W. A., Simpson, R. H., Blakeslee, R., & Durden, S. L. (1998). On the role of "hot towers" in tropical cyclone formation. *Meteorology and Atmospheric Physics*, *67*(1–4), 15–35. https://doi.org/10.1007/BF01277500

Sun, L., Tang, X., Zhuge, X., Tan, Z.-M., & Fang, J. (2021). Diurnal variation of overshooting tops in typhoons detected by Himawari-8 satellite. *Geophysical Research Letters*, *48*(21), e2021GL095565. https://doi.org/10.1029/2021GL095565

Tao, C., & Jiang, H. (2015). Distributions of shallow to very deep precipitation-convection in rapidly intensifying tropical cyclones. *Journal of Climate*, *28*(22), 8791–8824. https://doi.org/10.1175/JCLI-D-14-00448.1

Tao, C., Jiang, H., & Zawislak, J. (2017). The relative importance of stratiform and convective rainfall in rapidly intensifying tropical cyclones. *Monthly Weather Review*, *145*(3), 795–809. https://doi.org/10.1175/MWR-D-16-0316.1

Wang, Y., Rao, Y., Tan, Z. M., & Schönemann, D. (2015). A statistical analysis of the effects of vertical wind shear on tropical cyclone intensity change over the western North Pacific. *Monthly Weather Review*, *143*(9), 3434–3453. https://doi.org/10.1175/MWR-D-15-0049.1

Wu, C.-C., Tu, W.-T., Pun, I.-F., Lin, I.-I., & Peng, M. S. (2016). Tropical cyclone-ocean interaction in Typhoon Megi (2010)—A synergy study based on ITOP observations and atmosphere-ocean coupled model simulations. *Journal of Geophysical Research: Atmospheres*, *121*(1), 153–167. https://doi.org/10.1002/2015JD024198

Wu, Q., & Ruan, Z. (2016). Diurnal variations of the areas and temperatures in tropical cyclone clouds. *Quarterly Journal of the Royal Meteorological Society*, *142*(700), 2788–2796. https://doi.org/10.1002/qj.2868

Yang, H. L., Xiao, H., & Guo, C. W. (2015). Structure and evolution of a squall line in northern China: A case study. *Atmospheric Research*, *158*, 139–157. https://doi.org/10.1016/j.atmosres.2015.02.012

Yang, S., Bankert, R., & Cossuth, J. (2020). Tropical cyclone climatology from satellite passive microwave measurements. *Remote Sensing*, *12*(21), 3610. https://doi.org/10.3390/rs12213610

Yang, S., Lao, V., Bankert, R., Whitcomb, T. R., & Cossuth, J. (2021). Improved climatology of tropical cyclone precipitation from satellite passive microwave measurements. *Journal of Climate*, *34*(11), 4521–4537. https://doi.org/10.1175/JCLI-D-20-0196.1

Zagrodnik, J. P., & Jiang, H. (2014). Rainfall, convection, and latent heating distributions in rapidly intensifying tropical cyclones. *Journal of the Atmospheric Sciences*, *71*(8), 2789–2809. https://doi.org/10.1175/JAS-D-13-0314.1

Zipser, E., Zawislak, J., & Jiang, H. (2014). Necessary conditions for intensification of tropical cyclones: The role of mesoscale systems and convective intensity. WWOSC paper SCI-PS120.01.

Characteristics of Deep Convective Clouds, Precipitation, and Cloud Properties of Rapidly Intensifying Tropical Cyclones in the Western North Pacific

ORIGINALITY REPORT

14%	%	14%	%
SIMILARITY INDEX	INTERNET SOURCES	PUBLICATIONS	STUDENT PAPERS

PRIMARY SOURCES

1	Zuhang Wu, Yun Zhang, Lifeng Zhang, Hepeng Zheng. "Interaction of Cloud Dynamics and Microphysics During the Rapid Intensification of Super-Typhoon Nanmadol (2022) Based on Multi-Satellite Observations", Geophysical Research Letters, 2023 Publication	2%
2	Putu Aryastana, Chian-Yi Liu, Ben Jong-Dao Jou, Esperanza Cayanan, Jason Pajimola Punay, Ying-Nong Chen. "Assessment of Satellite Precipitation Data Sets for High Variability and Rapid Evolution of Typhoon Precipitation Events in the Philippines", Earth and Space Science, 2022 Publication	1%
3	Shun-Nan Wu, Brian J. Soden. "Signatures of Tropical Cyclone Intensification in Satellite Measurements of Ice and Liquid Water Content", Monthly Weather Review, 2017 Publication	1%

4	Keita Fujiwara, Ryuichi Kawamura, Tetsuya Kawano. "Remote Thermodynamic Impact of the Kuroshio Current on a Developing Tropical Cyclone Over the Western North Pacific in Boreal Fall", Journal of Geophysical Research: Atmospheres, 2020 Publication	1 %
5	Xinyan Zhang, Weixin Xu. "Is There an Outward Propagating Diurnal Signal in the Precipitation of Tropical Cyclones?", Geophysical Research Letters, 2022 Publication	1 %
6	Joseph P. Zagrodnik, Haiyan Jiang. "Rainfall, Convection, and Latent Heating Distributions in Rapidly Intensifying Tropical Cyclones", Journal of the Atmospheric Sciences, 2014 Publication	1 %
7	Putu Aryastana, Chian-Yi Liu, Ben Jong-Dao Jou, Esperanza Cayanan, Jason Pajimola Punay, Ying-Nong Chen. "Assessment of satellite precipitation datasets for high variability and rapid evolution of typhoon precipitation events in the Philippines", Earth and Space Science, 2022 Publication	1 %
8	Chian-Yi Liu, Chi-Hao Chiu, Po-Hsiung Lin, Min Min. "Comparison of Cloud-Top Property Retrievals From Advanced Himawari Imager,	<1 %

MODIS, CloudSat/CPR, CALIPSO/CALIOP, and Radiosonde", Journal of Geophysical Research: Atmospheres, 2020
Publication

---

9 Michael S. Fischer, Brian H. Tang, Kristen L. Corbosiero, Christopher M. Rozoff. "Normalized Convective Characteristics of Tropical Cyclone Rapid Intensification Events in the North Atlantic and Eastern North Pacific", Monthly Weather Review, 2018 <1%
Publication

---

10 S.-N. Wu, B. J. Soden, G. J. Alaka. "Ice Water Content as a Precursor to Tropical Cyclone Rapid Intensification", Geophysical Research Letters, 2020 <1%
Publication

---

11 Xinxi Wang, Haiyan Jiang, Oscar Guzman. "Relating Tropical Cyclone Intensification Rate to Precipitation and Convective Features in the Inner Core", Weather and Forecasting, 2023 <1%
Publication

---

12 Juan Huo, Yufang Tian, Xue Wu, Congzheng Han, Bo Liu, Yongheng Bi, Shu Duan, Daren Lyu. "Properties of ice cloud over Beijing from surface Ka-band radar observations during 2014–2017", Atmospheric Chemistry and Physics, 2020 <1%
Publication

13	Xinlei Han, Bin Zhao, Yun Lin, Qixiang Chen, Hongrong Shi, Zhe Jiang, Xuehua Fan, Jiandong Wang, Kuo-Nan Liou, Yu Gu. "Type-Dependent Impact of Aerosols on Precipitation Associated With Deep Convective Cloud Over East Asia", Journal of Geophysical Research: Atmospheres, 2022 Publication	<1 %
14	Naresh Krishna Vissa, P. C. Anandh, Venkata Sai Gulakaram, Gopinadh Konda. "Role and response of ocean–atmosphere interactions during Amphan (2020) super cyclone", Acta Geophysica, 2021 Publication	<1 %
15	Jialin Lin, Taotao Qian. "Rapid Intensification of Tropical Cyclones Observed by AMSU Satellites", Geophysical Research Letters, 2019 Publication	<1 %
16	Qianguang Tu, Zengzhou Hao. "Validation of Sea Surface Temperature Derived From Himawari-8 by JAXA", IEEE Journal of Selected Topics in Applied Earth Observations and Remote Sensing, 2020 Publication	<1 %
17	Xiang Wang, Haiyan Jiang, Jun A. Zhang, Ke Peng. "Satellite-observed warm-core structure	<1 %

in relation to tropical cyclone intensity change", Atmospheric Research, 2020
Publication

---

18 Liangxiao Sun, Xiaodong Tang, Xiaoyong Zhuge, Zhe-Min Tan, Juan Fang. "Diurnal Variation of Overshooting Tops in Typhoons Detected by Himawari-8 Satellite", Geophysical Research Letters, 2021 <1 %
Publication

---

19 Udai Shimada, Hiromi Owada, Munehiko Yamaguchi, Takeshi Iriguchi et al. "Further Improvements to the Statistical Hurricane Intensity Prediction Scheme Using Tropical Cyclone Rainfall and Structural Features", Weather and Forecasting, 2018 <1 %
Publication

---

20 Chian-Yi Liu, Chi-Hao Chiu, Po-Hsiung Lin, Min Min. "Comparison of Cloud-Top Property Retrievals from Advanced Himawari Imager, MODIS, CloudSat/CPR, CALIPSO/CALIOP, and radiosonde", Journal of Geophysical Research: Atmospheres, 2020 <1 %
Publication

---

21 William Miller, Hua Chen, Da-Lin Zhang. "On the Rapid Intensification of Hurricane Wilma (2005). Part III: Effects of Latent Heat of Fusion", Journal of the Atmospheric Sciences, 2015 <1 %
Publication

22	Zhenxin Ruan, Qiaoyan Wu. "Precipitation, Convective Clouds, and Their Connections With Tropical Cyclone Intensity and Intensity Change", Geophysical Research Letters, 2018 Publication	<1 %
23	Yuhao Liu, Shoude Guan, I-I Lin, Wei Mei, Fei-Fei Jin, Mengya Huang, Yihan Zhang, Wei Zhao, Jiwei Tian. "Effect of storm size on sea surface cooling and tropical cyclone intensification in the western north Pacific", Journal of Climate, 2023 Publication	<1 %
24	Rosimar Rios-Berrios, Ryan D. Torn, Christopher A. Davis. "An Ensemble Approach to Investigate Tropical Cyclone Intensification in Sheared Environments. Part II: Ophelia (2011)", Journal of the Atmospheric Sciences, 2016 Publication	<1 %
25	Udai Shimada, Takeshi Horinouchi. "Reintensification and Eyewall Formation in Strong Shear: A Case Study of Typhoon Noul (2015)", Monthly Weather Review, 2018 Publication	<1 %
26	Andrew T. Hazelton, Xuejin Zhang, Sundararaman Gopalakrishnan, William Ramstrom, Frank Marks, Jun A. Zhang. "HIGH-RESOLUTION ENSEMBLE HFV3 FORECASTS	<1 %

OF HURRICANE MICHAEL (2018): RAPID INTENSIFICATION IN SHEAR", Monthly Weather Review, 2020
Publication

---

27 Ke WANG, Guanghua CHEN, Xinxin BI, Donglei SHI, Kexin CHEN. "Comparison of Convective and Stratiform Precipitation Properties in Developing and Nondeveloping Tropical Disturbances Observed by the Global Precipitation Measurement over the Western North Pacific", Journal of the Meteorological Society of Japan. Ser. II, 2020 <1%
Publication

---

28 Jacob D. Carstens, Allison A. Wing. "Simulating Dropsondes to Assess Moist Static Energy Variability in Tropical Cyclones", Geophysical Research Letters, 2022 <1%
Publication

---

29 Jia Liang, Liguang Wu, Guojun Gu. "Rapid Weakening of Tropical Cyclones in Monsoon Gyres over the Tropical Western North Pacific", Journal of Climate, 2018 <1%
Publication

---

30 Jonathan Zawislak, Haiyan Jiang, George R. Alvey, Edward J. Zipser, Robert F. Rogers, Jun A. Zhang, Stephanie N. Stevenson. "Observations of the Structure and Evolution of Hurricane Edouard (2014) during Intensity <1%

Change. Part I: Relationship between the Thermodynamic Structure and Precipitation", Monthly Weather Review, 2016
Publication

31	K. Squires, S. Businger. "The Morphology of Eyewall Lightning Outbreaks in Two Category 5 Hurricanes", Monthly Weather Review, 2008 Publication	<1 %
32	Daniel P. Stern, David S. Nolan. "On the Height of the Warm Core in Tropical Cyclones", Journal of the Atmospheric Sciences, 2012 Publication	<1 %
33	J. Blunden. "State of the Climate in 2010", Bulletin of the American Meteorological Society, 06/2011 Publication	<1 %
34	Maximilien Patou, Jérôme Vidot, Jérôme Riédi, Guillaume Penide, Timothy J. Garrett. "Prediction of the Onset of Heavy Rain Using SEVIRI Cloud Observations", Journal of Applied Meteorology and Climatology, 2018 Publication	<1 %
35	Udai Shimada, Kazumasa Aonashi, Yoshiaki Miyamoto. "Tropical Cyclone Intensity Change and Axisymmetricity Deduced from GSMaP", Monthly Weather Review, 2017 Publication	<1 %

36	Carrasco, Cristina Alexandra, Christopher William Landsea, and Yuh-Lang Lin. "The Influence of Tropical Cyclone Size on Its Intensification", Weather and Forecasting Publication	<1 %
37	Donglei Shi, Guanghua Chen. "The implication of outflow structure for the rapid intensification of tropical cyclones under vertical wind shear", Monthly Weather Review, 2021 Publication	<1 %
38	Erin B. Munsell, Fuqing Zhang, Scott A. Braun, Jason A. Sippel, Anthony C. Didlake. "The Inner-Core Temperature Structure of Hurricane Edouard (2014): Observations and Ensemble Variability", Monthly Weather Review, 2018 Publication	<1 %
39	Hung-Chi Kuo, Satoki Tsujino, Chien-Chang Huang, Chung-Chieh Wang, Kazuhisa Tsuboki. "Diagnosis of the Dynamic Efficiency of Latent Heat Release and the Rapid Intensification of Supertyphoon Haiyan (2013)", Monthly Weather Review, 2019 Publication	<1 %
40	Islam, Tanvir, Prashant K. Srivastava, George P. Petropoulos, and Sudhir K. Singh. "Reduced major axis approach for correcting GPM/GMI	<1 %

radiometric biases to coincide with radiative transfer simulation", Journal of Quantitative Spectroscopy and Radiative Transfer, 2016.
Publication

---

41 Robert J. Bright. "Evidence of the Gulf Stream's influence on tropical cyclone intensity", Geophysical Research Letters, 2002 <1%
Publication

---

42 Saulo R. Freitas, Georg A. Grell, Angel D. Chovert, Maria Assunção F. Silva Dias, Ernani de Lima Nascimento. "A Parameterization for Cloud Organization and Propagation by Evaporation-Driven Cold Pool Edges", Journal of Advances in Modeling Earth Systems, 2024 <1%
Publication

---

43 Tsuneaki Suzuki. "Diurnal cycle of deep convection in super clusters embedded in the Madden-Julian Oscillation", Journal of Geophysical Research, 11/20/2009 <1%
Publication

---

44 Woojeong Lee, Sung-Hun Kim, Pao-Shin Chu, Il-Ju Moon, Alexander V. Soloviev. "An Index to Better Estimate Tropical Cyclone Intensity Change in the Western North Pacific", Geophysical Research Letters, 2019 <1%
Publication

---

45 Xinyan Zhang, Weixin Xu. "Diurnal Variations in Rainfall and Precipitation Asymmetry of <1%

Tropical Cyclones in the Northwest Pacific Region", Journal of Climate, 2021
Publication

---

46 Ziqiang Ma, Jintao Xu, Kang He, Xiuzhen Han, Qingwen Ji, TseChun Wang, Wentao Xiong, Yang Hong. "An updated moving window algorithm for hourly-scale satellite precipitation downscaling: A case study in the Southeast Coast of China", Journal of Hydrology, 2020 <1 %
Publication

---

47 Chuan-Chieh Chang, Chun-Chieh Wu. "On the Processes Leading to the Rapid Intensification of Typhoon Megi (2010)", Journal of the Atmospheric Sciences, 2017 <1 %
Publication

---

48 Chuanfeng Zhao, Yikun Yang, Yulei Chi, Yue Sun, Xin Zhao, Husi Letu, Yan Xia. "Recent progress in cloud physics and associated radiative effects in China from 2016 to 2022", Atmospheric Research, 2023 <1 %
Publication

---

49 Donglei Shi, Guanghua Chen. "Modulation of Asymmetric Inner-Core Convection on Midlevel Ventilation Leading up to the Rapid Intensification of Typhoon Lekima (2019)", Journal of Geophysical Research: Atmospheres, 2023 <1 %
Publication

50	Donglei Shi, Guanghua Chen. "Modulation of asymmetric inner-core convection on midlevel ventilation leading up to the rapid intensification of Typhoon Lekima (2019)", Journal of Geophysical Research: Atmospheres, 2023 Publication	<1 %
51	Gordon J. Labow. "Diurnal variation of 340 nm Lambertian equivalent reflectivity due to clouds and aerosols over land and oceans", Journal of Geophysical Research, 06/08/2011 Publication	<1 %
52	Haiyan Jiang, Joseph P. Zagrodnik, Cheng Tao, Edward J. Zipser. "Classifying Precipitation Types in Tropical Cyclones Using the NRL 37GHz Color Product", Journal of Geophysical Research: Atmospheres, 2018 Publication	<1 %
53	Hong, Xiaodong, Simon W. Chang, Sethu Raman, Lynn K. Shay, and Richard Hodur. "The Interaction between Hurricane Opal (1995) and a Warm Core Ring in the Gulf of Mexico", Monthly Weather Review, 2000. Publication	<1 %
54	Ibraheem Shayea, Tharek Abd Rahman, Marwan Hadri Azmi, Md. Rafiqul Islam. "Real Measurement Study for Rain Rate and Rain Attenuation Conducted Over 26 GHz	<1 %

Microwave 5G Link System in Malaysia", IEEE Access, 2018
Publication

55	Jae-Deok Lee, Chun-Chieh Wu, Kosuke Ito. "Diurnal Variation of the Convective Area and Eye Size Associated with the Rapid Intensification of Tropical Cyclones", Monthly Weather Review, 2020 Publication	<1 %
56	Jessica Blunden, Derek S. Arndt. "State of the Climate in 2018", Bulletin of the American Meteorological Society, 2019 Publication	<1 %
57	Lawrence, Miles B.. "Eastern North Pacific Hurricane Season of 1997", Monthly Weather Review, 1999. Publication	<1 %
58	Longsheng Liu, Yiwu Huang, Lian Liu. "Comparative analysis of the rapid intensification of two super cyclonic storms in the Arabian Sea", Tropical Cyclone Research and Review, 2024 Publication	<1 %
59	Michael S. Fischer, Paul D. Reasor, Robert F. Rogers, John F. Gamache. "An Analysis of Tropical Cyclone Vortex and Convective Characteristics in Relation to Storm Intensity	<1 %

using a Novel Airborne Doppler Radar Database", Monthly Weather Review, 2022
Publication

---

60 Qiaoyan Wu, Jiacheng Hong. "Diurnal Variations in Contraction of the Radius of Maximum Tangential Wind in Tropical Cyclones", Geophysical Research Letters, 2022
Publication

<1 %

---

61 Qiaoyan Wu, Zhenxin Ruan. "Rapid Contraction of the Radius of Maximum Tangential Wind and Rapid Intensification of a Tropical Cyclone", Journal of Geophysical Research: Atmospheres, 2021
Publication

<1 %

---

62 S. Kanada, H. Aiki. "Buffering Effect of Atmosphere–Ocean Coupling on Intensity Changes of Tropical Cyclones Under a Changing Climate", Geophysical Research Letters, 2023
Publication

<1 %

---

63 Shoujuan Shu, Xibin Feng, Daigao Teng. "Observed vertical structure of precipitation influenced by dry air for landfalling tropical cyclones over China", Journal of Geophysical Research: Atmospheres, 2021
Publication

<1 %

64	Si Gao. "Surface latent heat flux and rainfall associated with rapidly intensifying tropical cyclones over the western North Pacific", International Journal of Remote Sensing, 09/2010 Publication	<1 %
65	Song Yang, Vincent Lao, Richard Bankert, Timothy R. Whitcomb, Joshua Cossuth. "Improved Climatology of Tropical Cyclone Precipitation from Satellite Passive Microwave Measurements", Journal of Climate, 2021 Publication	<1 %
66	Wan-Ru Huang, Pin-Yi Liu, Ya-Hui Chang, Cheng-An Lee. "Evaluation of IMERG Level-3 Products in Depicting the July to October Rainfall over Taiwan: Typhoon Versus Non-Typhoon", Remote Sensing, 2021 Publication	<1 %
67	Weixin Xu, Steven A. Rutledge, Wenjuan Zhang. "Relationships between total lightning, deep convection, and tropical cyclone intensity change", Journal of Geophysical Research: Atmospheres, 2017 Publication	<1 %
68	Wenjuan Zhang, Yijun Zhang, Dong Zheng, Xiuji Zhou. "Lightning Distribution and Eyewall Outbreaks in Tropical Cyclones during Landfall", Monthly Weather Review, 2012	<1 %

Publication

69	Xiaomin Chen, Christopher M. Rozoff, Robert F. Rogers, Kristen L. Corbosiero et al. "Research Advances on Internal Processes Affecting Tropical Cyclone Intensity Change from 2018–2022", Tropical Cyclone Research and Review, 2023 Publication	<1 %
70	Xiaomin Chen, Yuqing Wang, Juan Fang, Ming Xue. "A Numerical Study on Rapid Intensification of Typhoon Vicente (2012) in the South China Sea. Part II: Roles of Inner-Core Processes", Journal of the Atmospheric Sciences, 2018 Publication	<1 %
71	Xidong Wang, Xin Wang, Peter C. Chu. "Air-sea interactions during rapid intensification of typhoon Fengshen (2008)", Deep Sea Research Part I: Oceanographic Research Papers, 2018 Publication	<1 %
72	Xinyan Zhang, Weixin Xu. "Strong Diurnal Pulsing of Cold Clouds in Rapidly Intensifying Tropical Cyclones", Geophysical Research Letters, 2021 Publication	<1 %
73	Zhanhong Ma, Xinyue Yan, Jianfang Fei. "Quantifying the Rightward Bias Extent of	<1 %

Tropical Cyclones' Cold Wakes", Geophysical Research Letters, 2023
Publication

74	"Clouds and their Climatic Impacts", Wiley, 2023 Publication	<1 %
75	Ganadhi Mano Kranthi, Medha Deshpande, K. Sunilkumar, Rongmie Emmanuel, S. T. Ingle. "Climatology and characteristics of rapidly intensifying tropical cyclones over the North Indian Ocean", International Journal of Climatology, 2022 Publication	<1 %
76	Hiu-fai Tam, Chun-wing Choy, Wai-kin Wong. "Development of objective forecast guidance on tropical cyclone rapid intensity change", Meteorological Applications, 2021 Publication	<1 %
77	Iam-Fei Pun, I.-I. Lin, Chun-Chi Lien, Chun-Chieh Wu. "Influence of the Size of Supertyphoon Megi (2010) on SST Cooling", Monthly Weather Review, 2018 Publication	<1 %
78	Qing Yan, Ting Wei, Zhongshi Zhang. "Variations in large-scale tropical cyclone genesis factors over the western North Pacific in the PMIP3 last millennium simulations", Climate Dynamics, 2016	<1 %

Publication

79	Murata, Akihiko. "The role of a convective burst in the genesis of typhoon Hagupit (2008) : CONVECTIVE BURST IN TYPHOON GENESIS", Journal of Geophysical Research Atmospheres, 2013. Publication	<1 %
80	Shizuo Fu, Richard Rotunno, Jinghua Chen, Xin Deng, Huiwen Xue. "A large-eddy simulation study of deep-convection initiation through the collision of two sea-breeze fronts", Atmospheric Chemistry and Physics, 2021 Publication	<1 %

Exclude quotes	On	Exclude matches	Off
Exclude bibliography	On		

Characteristics of Deep Convective Clouds, Precipitation, and Cloud Properties of Rapidly Intensifying Tropical Cyclones in the Western North Pacific

GRADEMARK REPORT

FINAL GRADE

/0

GENERAL COMMENTS

PAGE 1

PAGE 2

PAGE 3

PAGE 4

PAGE 5

PAGE 6

PAGE 7

PAGE 8

PAGE 9

PAGE 10

PAGE 11

PAGE 12

PAGE 13

PAGE 14

PAGE 15

PAGE 16